Mar Biol (2007) 152:395–404
DOI 10.1007/s00227-007-0694-0

RESEARCH ARTICLE

Photobiology of endolithic microorganisms in living coral skeletons: 1. Pigmentation, spectral reflectance and variable chlorophyll fluorescence analysis of endoliths in the massive corals *Cyphastrea serailia, Porites lutea* and *Goniastrea australensis*

P. J. Ralph · A. W. D. Larkum · M. Kühl

Received: 11 July 2006 / Accepted: 2 April 2007 / Published online: 25 April 2007
© Springer-Verlag 2007

Abstract We used microscopy, reflectance spectroscopy, pigment analysis, and photosynthesis-irradiance curves measured with variable fluorescence techniques to characterise the endolithic communities of phototrophic microorganisms in the skeleton of three massive corals from a shallow reef flat. Microscopic observations and reflectance spectra showed the presence of up to four distinct bands of photosynthetic microorganisms at different depths within the coral skeleton. Endolithic communities closer to the coral surface exhibited higher photosynthetic electron transport rates and a green zone dominated by *Ostreobium quekettii* nearest the surface had the greatest chlorophyll pigment concentration. However, *Ostreobium* was also present and photosynthetically active in the colourless band between the coral tissue and the green band. The spectral properties and pigment density of the endolithic bands were also found to closely correlate to photosynthetic rates as assessed by fluorometry. All endolithic communities were extremely shade-adapted, and photosynthesis was saturated at irradiances <7 μmol photons $m^{-2}s^{-1}$.

Communicated by G.F. Humphrey.

P. J. Ralph (✉)
Institute for Water and Environmental Resource Management,
Department of Environmental Sciences,
University of Technology, Sydney, Broadway,
2007 Sydney, NSW, Australia
e-mail: Peter.Ralph@uts.edu.au

A. W. D. Larkum
School of Biological Sciences, University of Sydney,
2006 Sydney, NSW, Australia

M. Kühl
Marine Biological Laboratory, Institute of Biology,
University of Copenhagen, Strandpromenaden 5,
3000 Helsingør, Denmark

Abbreviations

ANOVA	Analysis of variance
CCD	Charge coupled device
Chl	Chlorophyll
E_b	Photoinhibition index
E_d	Downwelling irradiance
E_k	Minimum saturating irradiance
E_m	Irradiance at maximum photosynthetic rate
ETR	Electron transport rate
F_m	Maximum fluorescence in dark
$F_{m'}$	Maximum fluorescence in light
F_o	Minimum fluorescence in dark
F_t	Minimum fluorescence in light
LED	Light emitting diode
PAR	Photosynthetically active radiation
P_m	Photosynthetic capacity at saturating irradiance
P_s	Scaling factor
PSII	Photosystem II
$rETR_{max}$	Relative maximum electron transport rate
RLC	Rapid light curve
α	Initial slope of RLC
β	Slope of RLC after photoinhibition
ϕ_{PSII}	Effective quantum yield

Introduction

Endolithic algae and bacteria inhabit the skeletons of living scleractinian corals. Most hermatypic corals (98%) contain

endolithic green algae and cyanobacteria, which often occur as discrete bands, at various depths in the skeletal matrix below the living coral surface (Le Campion-Alsumard et al. 1995). The most common endolithic alga is the siphonalean chlorophyte, *Ostreobium quekettii* (Phyllosiphoniaceae); which forms conspicuous green bands, running parallel to the coral surface. Lukas (1974) described two species of *Ostreobium* in Atlantic and Pacific reef corals: *O. quekettii* was common in corals from all geographic regions, whereas *O. constrictum* was only found in Caribbean corals and co-occurred with *O. quekettii*. Other endolithic organisms include cyanobacteria (e.g. *Plectonema tenebrans*), conchocelis stages of red algae (Bangiophycean rhodophytes), fungi and bacteria (Lukas 1974; Le Campion-Alsumard et al. 1995).

Endolithic algae were originally thought to be a significant component in the overall productivity of the reef ecosystem (Odum and Odum 1955). However, subsequent work has indicated that endolithic algae play a lesser role (Bellamy and Risk 1982; Schlichter et al. 1997). Nevertheless, they make a direct contribution to the reef food web. They are consumed by corallivorous grazers such as parrot fish and sea urchins, and also provide photosynthate to the coral (Schlichter et al. 1997). The latter may temporarily alleviate the lack of carbon sources for bleached corals that have lost their zooxanthellae symbionts (Fine and Loya 2001). Endolithic algae are adapted to extremely low-light conditions, limited exchange of gases, solutes and particulate matter between the surrounding water column and the skeleton matrix, and they consequently have low metabolic rates (Shashar et al. 1997). The diurnal gas exchange of endolithic algae is influenced by the metabolic activity of the coral, the zooxanthellae and the physical structure of the skeleton. Porewater within coral skeletons have a pH range of 8.2–8.3 (Shashar and Stambler 1992). Oxygen produced by photosynthesis inside coral skeletons can lead to supersaturation (M. Kühl, unpublished data). Microbial respiration in the dark lowers the pH and oxygen and increases nutrient content within coral porewater (Risk and Müller 1983). Endolithic algae can account for ~6% of the total oxygen production of the coral community, whilst endolith respiration accounted for only 1.4% of the colony's total oxygen consumption (Schlichter et al. 1997).

The photosynthetically active radiation (PAR) available to endolithic organisms is reduced in both quantity and quality as light penetrates the coral skeleton. Light is absorbed and scattered by zooxanthellae, host tissue, and the inorganic calcium carbonate skeleton. The remaining light penetrating to the endolithic algae is extremely attenuated, and the photosynthetic productivity of the endolithic region is relatively low (Shashar and Stambler 1992).

Estimated light levels reaching the endolithic organisms range from 2 to 10^{-6}% of surface irradiance (Halldal 1968), whilst the *Ostreobium* zone usually receives less than 1% (Shashar and Stambler 1992). This wide range reflects the use of different light measuring methodology and the heterogeneity in skeleton structure amongst corals. Coral skeleton is a highly scattering medium, and this complicates accurate quantification of light levels (Kühl 2005). Magnusson et al. (2006) presented a detailed study of the spectral light microclimate in coral skeleton showing that light penetration is strongly wavelength-dependent. Endolithic algae can absorb the red and far-red wavelengths, which reach levels of >2% of incident irradiance as opposed to <0.1% of PAR, as those wavelengths are not used by the zooxanthellae (Fork and Larkum 1989; Koehne et al. 1999; Magnusson et al. 2006). Low transmittance to the *Ostreobium* zone of the 650–680 nm bandwidth is attributed to Chl *a* absorption by zooxanthellae, while peridinin and carotenoids in conjunction with Chl *a* and *c* attenuate the light in the 400–500 nm range (Kühl et al. 1995). Significant light penetration of the longer wavelengths (such as far-red and near infra-red) are limited to the upper 15 m of the ocean; however, endolithic algae have been found at depth over 80 m and the general importance and adaptive value of far-red absorbing pigments thus remains controversial (Schlichter et al. 1997; Magnusson et al. 2006).

The light compensation point for *Ostreobium* has been found to be 10–50 µmol photons $m^{-2}s^{-1}$ and saturation occurred at 35–200 µmol photons $m^{-2}s^{-1}$ (Vooren 1981; Shashar and Stambler 1992; Schlichter et al. 1997). Photoinhibition of endoliths has been found to occur at ~100 µmol photons $m^{-2}s^{-1}$ (Schlichter et al. 1997). However, such high irradiances would only be experienced by endolith communities of corals in very shallow waters and/or in coral skeleton with bleached or damaged coral tissue (Fine et al. 2005).

Endolithic algae appear to form distinct bands within the coral skeleton. *Ostreobium* is found adjacent to the living coral, but its greatest density is usually deeper in the skeleton (5–30 mm deep), where it forms a green band parallel to the coral surface (Halldal 1968). Only the ''most peripheral'' green band was found by Halldal (1968) to be photosynthetically active. Shibata and Haxo (1969) suggested that light reaching the outer green band was only just sufficient to support photosynthesis, and therefore, the deeper bands were thought to be moribund. Multiple green bands were found in dead corals by Le Campion-Alsumard et al. (1995). However, they found that deeper bands were formed by cyanobacteria such as *Plectonema terebrans*. A ''white'' band in between the green and the coral tissue contained *Ostreobium*, and it was speculated that *Ostreobium* was photoinhibited at the higher PAR levels present in this outer region of the skeleton (Lukas 1974; Highsmith 1981). Corals growing at greater depth have green bands closer to the coral surface (Highsmith 1981).

While endolithic communities in coral skeleton have been known for many years (e.g. Duerden 1902), the diversity and ecophysiology of endolithic phototrophs are still an under-explored area, especially in terms of direct measurements of the physical and chemical microenvironment and the activity of endoliths inside the skeleton. In this study, we investigated the photobiology of endolithic microorganisms occurring within a medial longitudinal profile through colonies of three massive corals (*Cyphastrea serailia*, *Porites lutea* and *Goniastrea australensis*). We mapped the spatial distribution of endoliths via microscopy, pigment analysis and spectral reflectance characteristics, and characterised the photosynthetic performance by fine scale measurements of variable chlorophyll fluorescence.

Materials and methods

Coral samples

Coral samples collected from the reef flat of Heron Island Lagoon (152°6′E, 20°29′S) were maintained in flow-through aquaria for 2 days under shaded conditions (<100 µmol photons $m^{-2}s^{-1}$) prior to experiments. Sampling occurred during the austral summer, January 2001. Three species of shallow-water massive corals were investigated: *Cyphastrea serailia* (Forskål), *Porites lutea* (Edwards & Haime) and *Goniastrea australensis* (Edwards & Haime). Samples were cut in half by medial longitudinal section, using a diamond-tipped saw fitted with a 10 cm blade in shaded conditions, under continuous flushing of seawater. Once each sample was cut, it was placed in an aquarium on a sheet of black plastic to prevent light penetration through the cut surface. Samples were cut through the point of attachment and perpendicular to the coral surface; this ensured that the samples were vertically orientated. We were unable to bring isolates of *Ostreobium* into culture. However, from observations using light microscopy and epifluorescence microscopy at ×1000, we identified this alga as *Ostreobium quekettii* (sensu Lukas 1974).

Absorption spectra of pigments

Sections of coral skeleton were cut out using a high-speed hobby drill (Dremel, USA) with a carbide cutting tool, the section was crushed in acetone, centrifuged at 5,000 rpm for 5 min, and the supernatant was separated and used for pigment analyses. Chlorophyll concentration was determined using the method of MacKinney (1941).

Reflectance measurements

Reflectance spectra of living endolithic algae were measured with fiber-optic radiance microprobes on medial longitudinal sections of coral samples (Salih et al. 2000). A field radiance microprobe tapered to a tip diameter of 40 µm (Kühl and Jørgensen 1992; Kühl 2005) was connected to a sensitive fiber-optic diode array spectrometer (300–800 nm range, PMA-11 Hamamatsu Photonics, Japan; 1 nm spectral resolution). The radiance microprobe was positioned with a micromanipulator at a distance from the skeleton surface which resulted in light collection from an area with a diameter of ~0.2 mm. Samples were illuminated using a fiber-optic (1 mm quartz fiber) UV–VIS metal halide light (Tri-Lite-Z, World Precision Instruments, USA) equipped with a collimating lens. Spectra were corrected for dark current and varying exposure times. Spectra were normalised to a reflectance standard ($BaSO_4$-LabLeader White Reflectance Standard, Eastman-Kodak, USA). When large amounts of fluorescing pigment were present, the measured spectra contained information about both reflectance and fluorescence characteristics of the surface investigated.

Photosynthetic electron transport versus irradiance

Photosynthetic activity was assessed by measuring rapid light curves (RLC) of photosynthetic electron transport (Schreiber et al. 1997; Ralph and Gademann 2005), where samples were exposed to eight incremental steps (each of 10 s duration) of irradiance ranging from 0 to 20 µmol photons $m^{-2}s^{-1}$ using a 140 µm fiber-optic probe (Microfiber-PAM, Walz GmbH, Effeltrich, Germany; Schreiber et al. 1996). Relative electron transport rate (rETR) was determined according to the following formula: $rETR = \phi_{PSII} \times PAR$, where $\phi_{PSII} = (F_{m'} - F_t)/F_{m'}$ is the effective PSII quantum yield and PAR is the photosynthetic active radiation (Genty et al. 1989). The initial ϕ_{PSII} determination was measured in pseudo-darkness and the corresponding F and $F_{m'}$ values were used in Fig. 3 as proxies for F_o and F_m, whilst recognizing that these are not true dark-adapted values.

For quantitative comparison, the RLC's were characterised by several descriptive parameters such as photosynthetic efficiency under limiting light (α), minimum saturating irradiance (E_k) and $rETR_{max}$ (Kühl et al. 2001; Ralph et al. 2002). Data were exported from WinControl into Sigmaplot 2001 (v7.0, SPSS Inc.) where the ''Regression Wizard'' was used to fit a curve to the RLC. Empirical data were mathematically fitted to a double exponential function (Platt et al. 1980):

$$P = P_s\left(1 - e^{-(\alpha E_d/P_s)}\right)e^{-(\beta E_d/P_s)} \quad (1)$$

In the absence of photoinhibition ($\beta = 0$), the function becomes a standard rectangular hyperbola, with an

asymptotic maximum rETR value (Harrison and Platt 1986), and Eq. 1 can be simplified to:

$$P = P_m\left(1 - e^{-(\alpha E_d/P_m)}\right) \quad (2)$$

In Eq. 1, P_s is a scaling factor, defined as the maximum potential rETR in the absence of photoinhibitory processes, while P_m is the photosynthetic capacity at saturating light, α is the initial slope of the RLC before the onset of saturation, E_d is the downwelling irradiance (400–700 nm), and β characterises the slope of the RLC beyond the onset of photoinhibition. The parameters $rETR_{max}$, E_m and E_k were estimated using the following equations:

$$rETR_{max} = P_s\ (\alpha/(\alpha+\beta))(\beta/(\alpha+\beta))^{\beta/\alpha} \quad (3)$$

$$E_m = P_s/\alpha\ \log_e((\alpha+\beta)/\beta)) \quad (4)$$

$$E_k = ETR_{max}/\alpha \quad (5)$$

Cardinal points of the RLC's were analysed by a one-factor ANOVA (Sokal and Rohlf 1995). Differences between means were determined using the Tukey's HSD test with a *Bonferroni* adjustment (Systat v8.0).

Results

In each of the three species, *Cyphastrea serailia*, *Porites lutea* (Fig. 1) and *Goniastrea australensis*, we found a conspicuous dark-green pigmented zone at 2–15 mm beneath the living coral, sometimes separated from the coral tissue layer by a lighter zone. Microscopic observation with an epifluorescence microscope (Olympus BH-2) showed that the green layer contained both a green alga identified as *Ostreobium quekettii* and an unidentified filamentous cyanobacterium. Deeper inside the coral skeleton (~35 mm) and on a perimeter following that of the colony surface, we found in all three coral species another ~7 mm thick pale green layer separated from the first green layer by a colourless region ~10 mm wide. The pale green layer was dominated by an unidentified filamentous cyanobacterium. Deeper still and separated from the above layers by another colourless region, a third, pink layer ~7 mm thick was often, but not always observed. This layer contained an unidentified filamentous bacterium. Traces of bacteriochlorophylls were detected in the pigment analysis (data not shown) of this layer, indicating the presence of anoxygenic photosynthetic bacteria. In *Porites lutea*, a thin pale-blue layer with filamentous cyanobacteria was sometimes observed in specimens collected during the Austral summer. The band was found closer to the surface than the pink layer. The lowermost pink layer was near to the base of each specimen and it is possible that light reached this layer via the underside of the corals, and not by penetrating the coral skeleton from above.

Absorption spectra of extracted endolith pigments

Porites lutea and *Goniastrea australensis* had similar concentrations of Chl *a*, while *Cyphastrea serailia* had almost twice the concentration of chlorophyll within the *Ostreobium* green zone (Table 1; $P = 0.000$). Chlorophyll *a/b* ratios were similar across the three species of coral, ranging from 3 to 5. The chlorophyll *a* pigments were distributed across the various depth zones within the skeleton of *Porites lutea* (Table 2). The highest Chl *a* concentration was always found in the green *Ostreobium* zone. Cyanobacteria contain water soluble phycobiliproteins, which typically have a peak absorption at 560–590 nm and 620 nm. After various attempts at performing pigment extracts in aqueous buffer, we were still unable to quantitatively extract phycobiliproteins from endolith tissue samples, presumably because phycobiliproteins were irreversibly bound to the carbonate skeletal material during the attempted extractions. In extracts from the deepest pink zone in *P. lutea* we found a small but distinct absorption peak at ~800 nm (data not shown), indicating the presence of bacteriochlorophyll *a*—containing anoxygenic photosynthetic bacteria.

Reflectance measurements

The coral tissue in all three species exhibited a typical spectral reflectance pattern of symbiotic dinoflagellates with a high attenuation (low reflectance) from 400 to 550 nm, a trough between 550 and 600 nm and a chlorophyll reflectance minimum (=absorbance maximum) at ~670 nm. The trough was also present within the white zones. In the coloured zones below the surface, there were

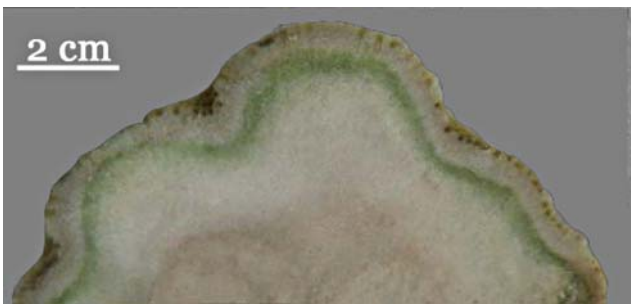

Fig. 1 Photograph of medial longitudinal section through a colony of *Porites lutea*, showing the distinct band of green endolithic algae (*Ostreobium* sp.) about 5 to 10 mm below the brown layer of zooxanthellae at the surface of the colony. The specimen is oriented with the top of the image being the upper surface

Table 1 Chlorophyll concentration and chlorophyll *a/b* ratio of the first green zone from three coral species

Coral	Total Chl	Chl *a/b* ratio	*n*
Porites lutea	8.99 ± 2.82	2.83 ± 1.26	5
Cyphastrea serailia	25.14 ± 7.21*	4.29 ± 1.92	5
Goniastrea australensis	10.96 ± 4.28	3.62 ± 0.39	7

Units are μg Chlorophyll cm^{-2}. Mean ± SEM

* Significantly different at $\alpha = 0.05$

Table 2 Chlorophyll *a* concentrations for *Porites lutea* endolithic organisms from four zones. Mean ($n = 2$)

Zone	Chl *a* (cm^{-2})	Chl *a* (cm^{-3})
First green	18.0	157.5
Second green	5.1	35.6
Inner blue	2.7	18.6
Inner pink	4.9	17.5

distinct reflectance minima (absorption peaks) at ~540 nm and often at ~600 nm, as well as the strong chlorophyll signal at ~670 nm.

Porites lutea showed differences in reflectance spectra from the four endolithic zones (Fig. 2b). The deepest zone (brown) showed an overall high reflectance and therefore low attenuation of light below 670 nm. The first green *Ostreobium* zones in *P. lutea* and *Cyphastrea serailia* samples had a shoulder in the reflectance spectrum at 650 nm, due to the presence of Chl *b*. The *P. lutea* white 1 and white 2 bands exhibited similar spectral reflectance, but the second zone had an overall lower absorbance. The two white zones in *C. serailia* were less similar. All zones in the *Goniastrea australensis* (Fig. 2c) samples showed a strong red Chl *a* peak at 678 nm. A fluorescent band in *G. australensis* had a distinct emission peak at 510 and 555 nm, seen as sharp troughs in the spectra.

Rapid light curves

The photosynthetic efficiency was progressively reduced in the deeper endolithic zones within the *Cyphastrea serailia* skeleton (Fig. 3), where the second white zone had a significantly lower efficiency than the deeper pigmented zones ($F = 5.5$, $P = 0.024$). The distribution of photosynthetic pigments can be inferred from the minimum fluorescence yield (F_o) from each zone. On examination of F_o and F_m data, it was apparent that a significant increase in the overall signal occurred within the green zone ($F = 61.2$, 35.0 $P = 0.000$, 0.000, respectively). The first white zone in *Cyphastrea serailia* had a higher effective quantum yield than the green zone, albeit the green zone had a fluorescence signal (F_o) up to four times that in the white zone.

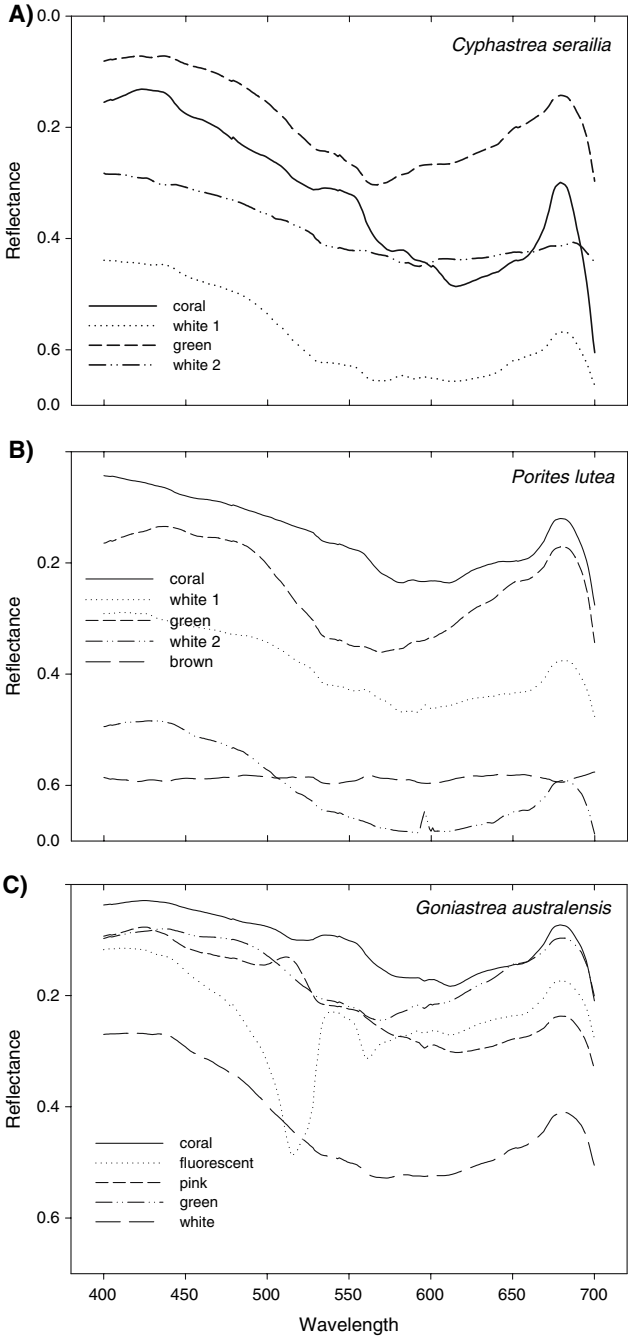

Fig. 2 In vivo reflection spectra (400–700 nm) of **a** *Cyphastrea serailia* **b** *Porites lutea* and **c** *Goniastrea australensis* tissue and associated endolith-containing layers in the skeleton. The scale has been inverted. Regions of low reflectance thus appear as peaks corresponding to absorption maxima, while regions of high reflectance appear as troughs in the spectra

Porites lutea (Fig. 3b) showed a similar chlorophyll fluorescence distribution to *C. serailia*, where the brown deepest zone was similar to the second white, with substantially lower apparent chlorophyll density (inferred from F_o; $F = 9.4$, $P = 0.001$), and a low effective quantum yield

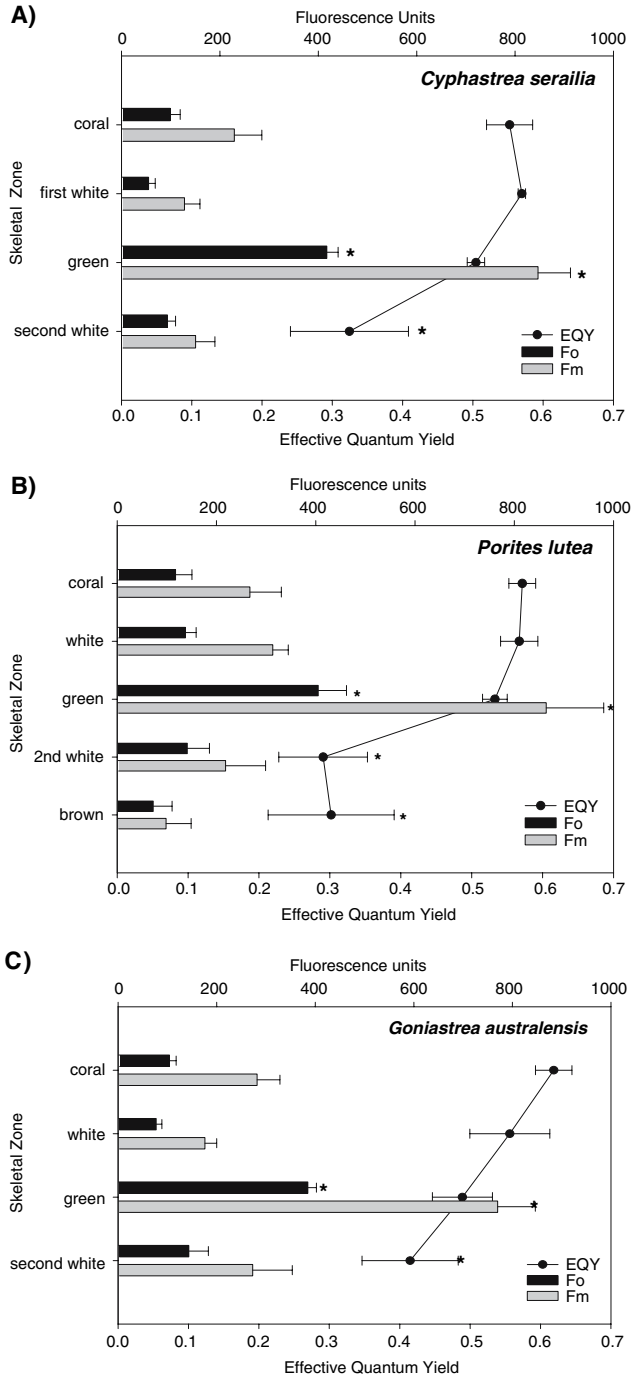

Fig. 3 **a–c** Horizontal bar graph of fluorescence (F_o), maximum fluorescence (F_m) and effective quantum yield ($\Delta F/F_{m'}$) from zones within the coral skeleton of **a** *Cyphastrea serailia*, **b** *Porites lutea* and **c** *Goniastrea australensis*. *Error bars* are standard error of mean ($n = 5$). *Asterisks* indicate mean values that were significantly ($\alpha < 0.05$) different from the remaining tissue zones

($F = 20.5$, $P = 0.000$). *Goniastrea australensis* (Fig. 3c) also showed a similar overall pattern, with a greater decline in effective quantum yield through each progressive depth zone. The green zone, once again had significantly ($F = 10.8$, $P = 0.001$) higher F_o (and F_m) signals.

To understand the photosynthetic capacity of the endolithic organisms, a series of rapid light curves were measured. Since we were characterizing shade-adapted endolithic algae, the irradiances used in the RLC's were optimised for low-light conditions, and RLC data relating to coral tissue were provided only for comparative purposes. The endosymbionts in the coral tissue from all three species were not saturated under the irradiance conditions provided during the measurements (Fig. 4) as the highest experimental irradiance was only 20 µmol photons $m^{-2}s^{-1}$.

The maximum relative electron transport rate ($rETR_{max}$) for the endolithic zones occurred at irradiances less than 7 µmol photons $m^{-2}s^{-1}$. The first white band inside *Cyphastrea serailia* showed the onset of photosynthesis saturation (E_k) at an irradiance of about 6.8 µmol photons $m^{-2}s^{-1}$, whilst in the remaining zones we found E_k values <2 µmol photons $m^{-2}s^{-1}$ (Fig. 4a; Table 3). The $rETR_{max}$ was progressively lower for each deeper zone. In *Cyphastrea serailia*, the $rETR_{max}$ of the white zone was ~2.6, whereas that of the green layer was 1.04 and of the second white was 0.45. The slopes of the light-limited region (α) of the three zones in *C. serailia* were not significantly different (Table 3).

The first band within *Porites lutea* exhibited a lower $rETR_{max}$ than the similar band within *C. serailia* (Fig. 4b; Table 3). The coral tissue of *P. lutea* was also not saturated by the RLC. The first white zone had an $E_k = 5.8$ µmol photons $m^{-2}s^{-1}$, whilst all other zones within this coral showed an $E_k < 3$ µmol photons $m^{-2}s^{-1}$ (Table 3). The $rETR_{max}$ for *P. lutea* was generally less than *Cyphastrea serailia*, being between 0.4 and 1.8. The endolithic bands within *Goniastrea australensis* were similar in $rETR_{max}$ and E_k to *C. serailia* (Fig. 4c; Table 3). The only substantial difference was the lack of the brown band, while all other bands were similar.

Discussion

We applied a range of new techniques to describe the distribution and activity of endolithic phototrophs within the skeleton of three corals. The process of cutting the coral skeleton may introduce cross-contamination of tissue from one endolithic zone to the next by smearing cells over the cut surface (Schlichter et al. 1997). However, if significant smearing had occurred, the fluorescence yields (F_m and F_o) would be more variable as the response would be an average mixture from all zones, which is clearly not the case (Figs. 3a–c). Therefore, we regard the impact of cross-contamination from the process of sectioning on our data as minor, if it has any significance at all.

Our observations of the endolithic community within living corals are similar to the observations of Le Campion-

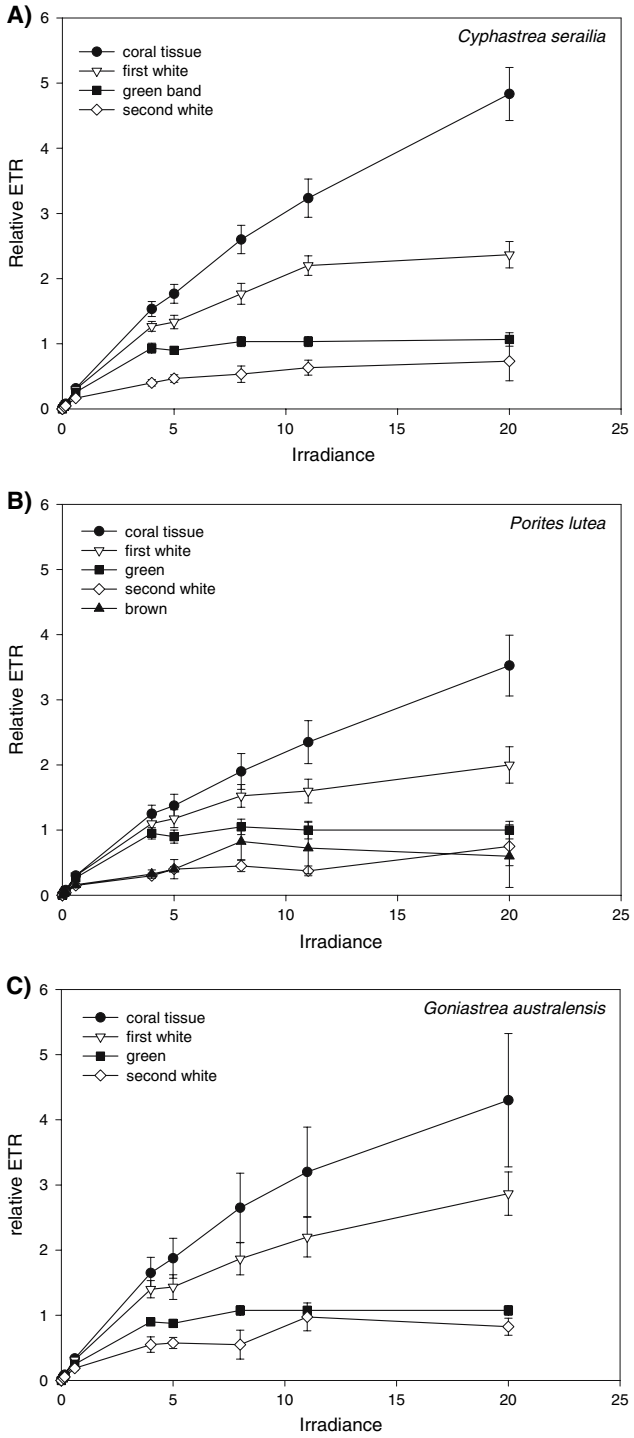

Fig. 4 **a–c** Rapid light curves of zones within *Cyphastrea serailia* containing endolithic algae (**a**), *Porites lutea* (**b**) and *Goniastrea australensis* (**c**). Curves are the average of replicate curves. Units of irradiance are µmol photons $m^{-2}s^{-1}$ and relative ETR are arbitrary units. *Error bars* are standard error of mean (n = 5)

Alsumard et al. (1995) made on dead corals, but differ from the observations of the same authors made in living corals. Le Campion-Alsumard et al. (1995) found *Ostreobium quekettii* only penetrating upwards within the skeleton of living corals, and they speculated that rapid coral growth was the reason that other algal communities did not become established. Our corals were collected from shallow areas of the Heron Island reef flat, where water movement is limited and high irradiances prevail. Under these circumstances the coral growth may have been slower and light penetration into the coral skeleton relatively higher, as compared to the corals studied by Le Campion-Alsumard et al (1995). Our observations of several endolihic bands are in line with other studies (Halldal 1968; Lukas 1974; Highsmith 1981). However, we observed for the first time the spectral signatures of cyanobacteria and Bchl-containing anoxygenic photosynthetic bacteria in the deeper zones of the skeletons of living corals. Our finding confirm those of Magnusson et al. (2006), who investigated the light microenvironment inside coral skeleton.

Pigments and spectral reflectance of endoliths

Ostreobium contains Chl *a* and *b*, α-carotene and Siphonales-specific xanthophyll pigments (Jeffrey 1968). Chlorophyll *a* concentrations found in the first green zone (Table 1) within *Goniastrea australensis* showed that the *Ostreobium* dominated zone had twice the chlorophyll level found in the other two species. A Chl *a/b* ratio of about 3 is normal for shade-adapted higher plants, whereas deep shade-adapted *Ostreobium* can have a ratio of 1.3–1.5 (Halldal 1968; Jeffrey 1968). Schlichter et al. (1997) found endolithic communities within shallow samples of *Mycedium elephantotus* to have a Chl *a/b* ratio of 2.8. We found Chl *a/b* ratios of 2.8–4.3 in our samples. Given that our corals were collected from a shallow lagoon, it is likely that the relatively high Chl *a/b* ratios were due to the fact that the *Ostreobium* was less shade-adapted and that cyanobacteria (with only Chl *a*) were also present, especially in *G. australiensis* and *C. serailia*. In the deeper endolithic bands Chl *b* was not measurable, suggesting, along with the reflectance spectra, that the organisms here were predominantly cyanobacteria. However, the lower absolute levels of Chl *a* in the deeper bands also indicates a reduced level of photosynthetic activity, which was supported by the variable fluorescence analysis and oxygen production studies (Kühl et al., unpublished data).

Our reflectance spectra (Fig. 2) showed the presence of Chl *a* in all zones including the white zone on either side of the uppermost green band. Reflectance spectra of coral tissue clearly showed the presence of dinoflagellates (zooxanthellae) containing peridinin, as evident from a shoulder in the spectra at 540–550 nm. Since cyanobacteria may also be present on the carbonate skeleton near the surface (Le Campion-Alsumard et al. 1995), there may also

Table 3 Cardinal points from the RLC curve fitting for each zone within the coral colonies ($n = 5$)

Species	Cardinal	White 1	Green	White 2	Brown	P
Cyphastrea serailia	$rETR_{max}$	2.61 ± 0.09	1.04 ± 0.10	0.45 ± 0.01	–	0.008*
	E_k	6.87 ± 0.38	2.12 ± 0.13	1.08 ± 0.06	–	0.006*
	α	0.38 ± 0.01	0.49 ± 0.02	0.41 ± 0.02	–	0.208
Porites lutea	$rETR_{max}$	1.84 ± 0.37	1.03 ± 0.14	0.45 ± 0.03	0.41 ± 0.05	0.004*
	E_k	5.78 ± 1.00	1.96 ± 0.26	2.71 ± 0.24	2.86 ± 0.38	0.001*
	α	0.35 ± 0.01	0.52 ± 0.05	0.17 ± 0.02	0.14 ± 0.01	0.000*
Goniastrea australensis	$rETR_{max}$	2.59 ± 0.09	1.00 ± 0.09	0.44 ± 0.01	–	0.000*
	E_k	6.08 ± 1.07	2.62 ± 0.17	3.52 ± 0.84	–	0.023*
	α	0.36 ± 0.07	0.43 ± 0.04	0.25 ± 0.04	–	0.355

$rETR_{max}$ is arbitrary, α (is a ratio and E_k has units of μmol photons $m^{-2}s^{-1}$

* denotes significantly different treatments at $P < 0.05$

have been some contribution from phycobiliproteins absorbing at 560–620 nm. The presence of a distinct shoulder at 640 nm in the first green band indicates the presence of Chl *b* from the abundant *Ostreobium*, but again, as in all the innermost bands, there were absorption peaks around 550 and 600 nm indicating the presence of cyanobacterial phycobiliproteins.

A reduced and altered spectral absorbance in the deeper zones indicates a change in the endolithic community composition from mainly *Ostreobium* with Chl *a* and *b*, to a predominance of cyanobacteria containing Chl *a* and phycobiliproteins. To thrive under the optically dense coral tissue that exhibits a strong light attenuation and spectral filtering, the endolithic phototrophs seem optimised to exploit this cryptic environment by using wavelengths (550–630 nm and >700 nm) that transmit most efficiently (Koehne et al. 1999). When grown under low light conditions the *Ostreobium* sp. culture studied by Koehne et al. (1999) was shown to possess large quantities of far-red absorbing chlorophylls.

Fluorescent bands, as found in *G. australensis* (Fig. 2c) have been found in association with endolithic algae and can contain humic or fluvic acids from terrestrial run-off (Priess et al. 2000). The red-brown colouration found deep inside the *Porites lutea* specimens (Fig. 2b) could be associated with a cyanophyte (such as *Plectonema terebrans*; Le Campion-Alsumard et al. 1995), while a light-brown coloured deep skeleton layer is often related to the presence of chitinoclastic bacteria (Bak and Laane 1987). Delvoye (1992) found pink and red-coloured regions (Fig. 2c); however, this band requires further spectral characterisation. It should be noted that the present data represent reflectance at the cut surface of the corals, not transmission or absorbance through an uncut skeleton. Information on light transmission and absorptance in coral skeleton is scarce. However, the recent application of fiber-optic microprobes (Kühl 2005) in combination with micro-drilling of the skeleton has shown that <0.1–10% of the incident visible irradiance reaches the endolith layer, depending on the coral species and their skeleton structure, while 5–10 times more far-red and NIR light penetrates to the endoliths (Magnusson et al. 2006).

Photosynthetic activity of endoliths

We used variable chlorophyll fluorescence techniques to obtain curves of relative photosynthetic electron transport rate as a function of irradiance in endolithic phototrophs within corals. Our data clearly demonstrate that the endolithic phototrophs are extremely shade-adapted (Fig. 4a–c), showing saturation at light levels of a dimly lit room (<10 μmol photons $m^{-2}s^{-1}$). Generally, all three species showed a similar pattern, with the highest fluorescence signal in the green (*Ostreobium*) zone. Koehne et al. (1999) and others have postulated that long wavelength forms of chlorophyll (>700 nm) found in *Ostreobium* will increase the antenna absorption. Koehne et al. (1999) further suggested that this would result in the loss of photosynthetic efficiency. Effective quantum yield remained above 0.5 for the upper three zones (dominated by *Ostreobium*). This finding is supported by model calculations showing that under low-light conditions, the photosynthetic efficiency of PSII was maintained (Trissl 2003).

RLC's for all zones of *Cyphastrea serailia* and *Goniastrea australensis* were similar in shape, suggesting a similar light field, possibly linked to the presence of light guides in the skeleton (Highsmith 1981). We measured RLCs by applying irradiance to the endolith surface. However, it should be recognised that the spectrum delivered to the various layers may not be optimal for the various endoliths. Exposing the uncut surface of a coral to increasing irradiance while measuring the impact on the

endoliths on the undersurface would yield more realistic results, but is technically difficult to realise.

In a preliminary study, Grunwald and Kühl (2004) applied an imaging fluorometer to map rETR versus irradiance across a cut *Cyphastrea* sp. and showed a differentiation in rETR versus irradiance curves between coral tissue, the green *Ostreobium* layer and the white skeleton below this layer. However, they did not observe saturation of rETR at low irradiance. This was explained as an artefact of the imaging approach, where intense LED illumination can stimulate endolith activity in deeper layers at increasing levels of actinic light, while surface populations may be inhibited. In comparison, we used a microfibre for the fluorescence analysis, which measures the photosynthetic activity in close proximity to the fiber tip. Our results thus give a more realistic picture of the photosynthetic capacity of the endoliths.

Apart from the *Porites* white1 zone, all $rETR_{max}$ values were remarkable similar in all three species (Table 3). Endolithic communities growing deeper inside coral were adapted to lower light climates, resulting in a lower $rETR_{max}$, lower E_k and a higher photosynthetic efficiency (α) at limiting irradiance. Our data on the *Ostreobium* layer agree with data of Schlichter et al. (1997), who found *Ostreobium quekettii* to have an E_k of ~10 µmol photons $m^{-2}s^{-1}$. Halldal (1968) found similar patterns in the response of endolithic photosynthesis as a function of irradiance. In the upper region of the green band he found a typical sun-adapted curve, whilst samples taken from the middle of the green layer showed a classical shade response curve with an acute slope in the light-limiting region of the curve and a dramatic decline (photo-oxidation) at elevated irradiances. Samples from the bottom of the green layer did not respond to light; this was not dissimilar to the current results.

In this study, we used variable fluorescence measurements of effective quantum yield of the PSII charge separation to derive rETR as a proxy for photosynthesis. Whether rETR is indeed correlated with photosynthetic oxygen production of the endoliths remains to be investigated in more detail. This was the first application of optical sensors for 2-dimensional mapping of oxygen concentration in *Porites* sp. indicating that net oxygen production is induced in the *Ostreobium* layer already at <2 µmol photons $m^{-2}s^{-1}$ and apparently saturates around 30 µmol photons $m^{-2}s^{-1}$ (Kühl et al., unpublished data). Another promising approach for further photobiological studies of coral endoliths is based on the use of a combined microsensor for oxygen and chlorophyll fluorescence (Kühl 2005). Such a sensor has already been used in studies of coral tissues showing discrepancy between photosynthetic oxygen production and rETR at high irradiance (Ulstrup et al. 2006).

Conclusions

In conclusion, we have shown that the endolithic community of coral skeletons is composed of photosynthetic microorganisms with a wide diversity of pigments for capturing wavelengths that pass through the coral tissue and are transmitted through the skeleton. The three coral species investigated had similar endolithic communities, as shown by microscopic examination, pigmentation and photosynthesis-irradiance responses. Spectral properties and pigment density of the endolithic bands were found to closely correlate with photosynthetic rates, as assessed by fluorometry. All endolithic communities were extremely shade-adapted, and photosynthesis was saturated at irradiances less than 7 µmol photons $m^{-2}s^{-1}$.

Acknowledgments This study was supported by UTS Internal Funds, the Australian Research Council (PJR and AWDL) and the Danish Natural Science Research Council (MK). A. Glud is thanked for excellent technical assistance. We wish to thank the staff at Heron Island Research station for their support and assistance in this research. All work was carried out under Queensland National Parks and Wildlife Service collection permit G01/623. This is Contribution No. 2 of the Sydney Harbour Institute of Marine Science.

References

Bak RPM, Laane WPM (1987) Annual black bands in skeletons of reef corals (Scleractinia). Mar Ecol Prog Ser 38:169–175

Bellamy N, Risk MJ (1982) Coral gas: oxygen production in *Millipora* on the Great Barrier Reef. Sci NY 215:1618–1619

Delvoye L (1992) Endolithic algae in living stony corals: algal concentrations under influence of depth-dependent light conditions and coral tissue fluorescence in *Agarica agaricites* (L.) and *Meandrina meandrites* (L.) (Scleractina, Anthozoa). Stud Nat Hist Caribb Reg 71:24–41

Duerden JE (1902) Boring algae as agents in the disintegration of corals. Bull Am Mus Nat Hist 16:323–332

Fine M, Loya Y (2001) Endolithic algae: an alternative source of photoassimilates during coral bleaching. Proc R Soc Lond B 269:1205–1210

Fine M, Steindler L, Loya Y (2004) Endolithic algae photoacclimate to increased irradiance during coral bleaching. Mar Freshw Res 55:115–121

Fine M, Meroz-Fine E, Hoegh-Guldberg O (2005) Tolerance of endolithic algae to elevated temperature and light in the coral Montipora monasteriata from the southern Great Barrier Reef. J Exp Biol 208:75–81

Fork DC, Larkum AWD (1989) Light harvesting in the green alga *Ostreobium* sp., a coral symbiont adapted to extreme shade. Mar Biol 103:381–385

Genty B, Briantais JM, Baker NR (1989) The relationship between the quantum yield of photosynthetic electron transport and quenching of chlorophyll fluorescence. Biochim Biophys Acta 990:87–92

Grunwald B, Kühl M (2004) A system for imaging variable chlorophyll fluorescence of aquatic phototrophs. Ophelia 58:79–89

Halldal P (1968) Photosynthetic capacities and photosynthetic action spectra of endozoic algae of the massive coral *Favia*. Bull Mar Biol Lab Woods Hole 134:411–424

Harrison WG, Platt T (1986) Photosynthesis–irradiance relationships in polar and temperate phytoplankton populations. Polar Biol 5:153–164

Highsmith RC (1981) Lime-boring algae in hermatypic coral skeletons. J Exp Mar Biol 55:267–281

Jeffrey SW (1968) Pigment composition of Siphonales algae in the brain coral *Favia*. Biol Bull 135:141–148

Koehne B, Elli G, Jennings RC, Wilhelm C, Trissl H-W (1999) Spectroscopic and molecular characterization of a long wavelength absorbing antenna of *Ostreobium* sp. Biochim Biophys Acta 1412:94–107

Kühl M, Jørgensen BB (1992) Spectral light measurements in microbenthic phototrophic communities with a fiber-optic microprobe coupled to a sensitive diode array detector. Limnol Oceanogr 37:1813–1823

Kühl M, Cohen Y, Dalsgaard T, Jørgensen BB, Revsbech NP (1995) The microenvironment and photosynthesis of zooxanthellae in scleractinian corals studied with microsensors for O_2, pH and light. Mar Ecol Progr Ser 117:159–172

Kühl M, Lassen C, Revsbech NP (1997) A simple light meter for measurements of PAR (400–700 nm) with fiber-optic microprobes: application for P versus I measurements in microbenthic communities. Adv Microb Ecol 13:197–207

Kühl M, Glud RN, Borum J, Roberts R, Rysgaard S (2001) Photosynthetic performance of surface associated algae below sea ice as measured with a pulse amplitude modulated (PAM) fluorometer and O_2 microsensors. Mar Ecol Progr Ser 223:1–14

Kühl M (2005) Optical microsensors for analysis of microbial communities. In: Leadbetter JR (ed) Environmental microbiology. Meth Enzym 397:166–199

Le Campion-Alsumard T, Goubic S, Hutchings P (1995) Microbial endoliths in skeletons of live and dead corals: *Porites lobata* (Moorea, French Polynesia). Mar Ecol Progr Ser 117:149–157

Lukas KJ (1974) Two species of the chlorophyte genus *Ostreobium* from skeletons of Atlantic and Caribbean reef corals. J Phycol 10:331–335

MacKinney G (1941) Absorption of light by chlorophyll solutions. J Biochem 140:322–355

Magnusson SH, Fine M, Kühl M (2006) Light microclimate of endolithic phototrophs in the scleractian corals *Montipora monasteriata* and *Porites cylindrica*. Mar Ecol Progr Ser (in press)

Odum HT, Odum EP (1955) Trophic structure and productivity of a windward coral reef community on Eniwetok Atoll. Ecol Monogr 25:291–320

Platt T, Gallegos CL, Harrison WG (1980) Photoinhibition of photosynthesis in natural assemblages of marine phytoplankton. J Mar Res 38:687–701

Priess K, Le Campion-Alsumard T, Golubic S, Gadel F, Thomassin BA (2000) Fungi in corals: black bands and density-banding of *Porites lutea* and *P. lobata* skeleton. Mar Biol 136:19–27

Ralph PJ, Gademann R, Larkum AWD, Kühl M (2002) Spatial heterogeneity in active fluorescence and PSII activity of coral tissues. Mar Biol 141:639–646

Ralph PJ, Gademann R (2005) Rapid light curves: a powerful tool for the assessment of photosynthetic activity. Aquat Bot 82:222–237

Risk MJ, Müller HR (1983) Porewater in coral heads: evidence for nutrient regeneration. Limnol Oceanogr 28(5):1004–1008

Salih A, Larkum A, Cox G, Kühl M., Hoegh-Guldberg O (2000) Fluorescent pigments in coral are photoprotective. Nature 408:850–853

Schlichter D, Kampmann H, Conrady S (1997) Trophic potential and photoecology of endolithic algae living within coral skeletons. PSZN Mar Ecol 18:299–317

Schreiber U, Gademann R, Ralph PJ, Larkum AWD (1997) Assessment of photosynthetic performance of *Prochloron* in *Lissoclinum patella* by *in situ* and *in hospite* chlorophyll fluorescence measurements. Plant Cell Physiol 38:945–951

Schreiber U, Kühl M, Klimant I, Reising H (1996) Measurement of chlorophyll fluorescence within leaves using a modified PAM fluorometer with a fiber-optic microprobe. Photosynth Res 47:103–109

Shashar N, Stambler N (1992) Endolithic algae within corals—life in an extreme environment. J Exp Mar Biol Ecol 163:277–286

Shashar N, Banaszak AT, Lesser MP, Amrami D (1997) Coral endolithic algae: life in a protected environment. Pac Sci 51:167–173

Shibata K, Haxo FT (1969) Light transmission and spectral distribution through epi- and endozoic algal layers in the brain coral, *Favia*. Biol Bull 136:461–468

Sokal RR, Rohlf FJ (1995) Biometry: the principles and practice of statistics in biological research. 3rd edn. WH Freeman and Co. New York

Trissl H-W (2003) Modelling the excitation energy capture in thylakoid membranes. In: Larkum AWD, Douglas SE, Raven JA (eds) Photosynthesis in algae. Kluwer, Dordrecht, pp 245–276

Ulstrup KE, Ralph PJ, Larkum AWD, Kühl M (2006) Intra-colonial variability in light acclimation of zooxanthellae in coral tissues of *Pocillopora damicornis*. Mar Biol 149:1325–1335

Vooren CM (1981) Photosynthetic rates of benthic algae from the deep coral reef of Curacao. Aquat Bot 10:143–154